Differences In pH_i Recovery In CO_2-Chemosensitive And Non-Chemosensitive Cells: Predictions From A Mathematical Model

Juan M. Cordovez, Chris Clausen, Leon C. Moore, and Irene C. Solomon

***Abstract*—in this paper, we present a mathematic model designed to identify potential mechanisms responsible for the observed differences in pH_i recovery in CO_2-chemosensitive versus non-chemosensitive cells. The model suggests that differences in pH_i regulation may be dependent upon differences in the activation set-point of the internal modifier site of the Na^+/H^+ exchanger (NHE).**

I. Introduction

NUMEROUS studies have suggested that a decrease in intracellular pH (pH_i) is the primary stimulus for CO_2 sensing in central CO_2 chemoreceptors. In CO_2 chemosensitive neurons, an increase in CO_2 leads to a maintained reduction in pH_i while in non-chemosensitive neurons pH_i recovery is observed [1]. Regulation of pH_i in most cells is dependent upon the rate of CO_2 hydration/dehydration, intrinsic buffering capacity, Na^+/H^+ exchange (NHE), and $HCO3^-/Cl^-$ exchange (AE). Thus, increased levels of CO_2, which lead to the rapid hydration of CO_2 to H^+ and $HCO3^-$ (a reaction catalyzed by carbonic anhydrase, CA), result in a fall in pH_i, which is partially rapidly offset by intracellular buffering and transmembrane extrusion of H^+. Although the precise mechanism(s) for the differential regulation of pH_i recovery in CO_2 chemosensitive versus non-chemosensitive neurons remains to be identified, numerous *in vitro* studies have begun to evaluate the role of NHE in pH_i regulation in these cell populations [1-5]. These studies have demonstrated that functional NHE is necessary for pH_i recovery, and they suggest that impairment of normal NHE activity may be responsible for the lack of pH_i recovery in chemosensitive neurons [1-3]. An alternate explanation suggests that expression of different NHE isoforms may be responsible for this differential regulation, with the NHE-3 isoform, instead of the NHE-1 isoform (found in most neurons), playing a primary role in CO_2 sensing [4-5]. To evaluate these possibilities, we developed a mathematical model to investigate potential mechanisms participating in pH_i regulation in response to simulated hypercapnic acidosis. The current model extends the recent model proposed by Hempleman and Posner [6], which utilized a simplification of basic acid-base chemistry to assess mechanisms of pH_i regulation in intrapulmonary chemoreceptors (IPC), which show an inverse response to elevated levels of CO_2 (*i.e.*, high CO_2 decreases IPC discharge).

Manuscript received May 15, 2006. This work was supported by the National Institutes of Health under Grant DK66124.

J. M. Cordovez is with the Department of Biomedical Engineering, Stony Brook University, Stony Brook, NY 11794 USA. (e-mail: jcordove@ic.sunysb.edu).

C. Clausen is with the Department of Physiology and Biophysics, Stony Brook University, Stony Brook, NY 11794 USA. (E-mail: Chris.Clausen@sunysb.edu).

L. C. Moore is with the Department of Physiology and Biophysics, Stony Brook University, Stony Brook, NY 11794 USA. (E-mail: Leon.Moore@sunysb.edu).

I. C. Solomon is with the Department of Physiology and Biophysics, Stony Brook University, Stony Brook, NY 11794 USA. (Phone: 631-444-1043; fax: 631-444-3432; E-mail: Irene.Solomon@sunysb.edu).

II. Mathematical Model

The current model incorporates conservation of mass and electroneutrality constraints, kinetic models of the Na^+/K^+-ATPase, AE, NHE, and passive permeation pathways for ions, nonelectrolytes, and H_2O. H^+ buffering (both inside and out) is handled by multiple buffer species all subject to the isohydric principle. A more detailed description of the model is provided below:

A. State Equations and Buffers

Cell volume determined by water flux:

$$\frac{dV}{dt} = -AJ_w$$

Intracellular solute concentrations determined by solute and water fluxes:

$$\frac{V}{A}\frac{dC_i^i}{dt} = C_i^i J_w - J_i$$

where subscript i denotes solute species.

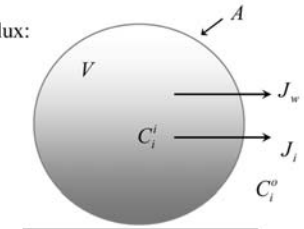

Cell where arrows denote positive flux.

Extracellular concentrations (C_i^o) are constant.

Total acid concentration (superscripts i and o omitted):

$$H_T = C_{H^+} + C_{H_2CO_3} + C_{H_2PO_4^-} + C_{NH_4^+}$$

Total buffer concentrations:

$$B_{bicarb} = C_{H_2CO_3} + C_{HCO_3^-}$$

$$B_{phosphate} = C_{H_2PO_4^-} + C_{HPO_4^{2-}}$$

$$B_{ammonia} = C_{NH_4^+} + C_{NH_3}$$

C_{H^+} must adhere to the isohydric principle, and is determined by solving numerically (e.g., Newton's method):

$$H_T = C_{H^+} + \sum_j \frac{C_{H^+} B_j}{C_{H^+} + K_a^j}$$, where j denotes buffer system.

Concentrations of other buffer species determined from respective B's and K_a's.

B. Solute and Water Fluxes

For nonelectrolytes, simple diffusion:

$$J_i^{passive} = P_i\left(C_i^i - C_i^o\right)$$

For electrolytes, ionic currents:

$$i_i = g_i\left(E_m - E_i\right)$$

where E_i is the Nernst potential

$$E_i = \frac{RT}{z_i F}\log_e\frac{C_i^o}{C_i^i}$$

Electrolyte fluxes given by

$$J_i^{passive} = \frac{i_i}{z_i F}$$

Membrane potential E_m is that that results in zero net current flow:

$$E_m = \frac{\left(\sum_i g_i E_i\right) - i_p}{\sum_i g_i}$$

(i_p is net pump current).

Water flux occurs via osmosis

$$J_w = P_w \sum_i \sigma_i\left(C_i^o - C_i^i\right)$$

Na^+-K^+ ATPase (sodium pump): cooperativity binding model

$$i_p = i_{max}\left[1+\left(\frac{K_K}{C_K^o}\right)^2\right]^{-1}\left[1+\left(\frac{K_{Na}}{C_{Na}^i}\right)^3\right]^{-1}$$

Na^+ and K^+ pump fluxes given by

$$J_{Na}^p = 3i_p/F \quad \text{and} \quad J_K^p = -2i_p/F$$

C. Hydration/Dehydration of CO_2

Bicarbonate buffer system described by:

$$CO_2 + H_2O \underset{k_d}{\overset{k_h}{\rightleftharpoons}} H_2CO_3 \overset{K_a}{\rightleftharpoons} H^+ + HCO_3^-$$

not in equilibrium ↑ k_d ; ↖ in equilibrium

Hydration of CO_2 results in a chemically-produced flux of H_2CO_3

$$J_{H_2CO_3}^{chem} = \frac{V}{A}\left(k_d C_{H_2CO_3}^i - k_h C_{CO_2}^i\right)$$

CO_2 readily permeable, constant throughout:

$$C_{CO_2}^o = C_{CO_2}^i = 0.03 \times P_{CO_2}$$

D. $HCO3^-/Cl^-$ and Na^+/H^+ Exchange

Anion exchanger: J^{exch}

Kinetics of anion exchanger by Chang and Fujita (*AJP Renal*, 281:F222, 2001): the transporter has a binding site that competes for Cl^- and HCO_3^-.

The transporter is in equilibrium resulting in a constant net flux (J_{net}, figure right).

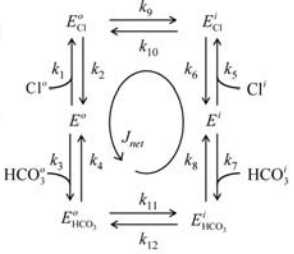

Rate constants (k_1–k_{12}) are appropriate for rat distal tubular cells. The values are thermodynamically consistent; zero net transport occurs when $C_{HCO_3^-}^o C_{Cl^-}^o = C_{HCO_3^-}^i C_{Cl^-}^i$.

The transporter also has an internal modifier site (not shown) that binds to Cl^- or HCO_3^-. Occupancy of the site effectively reduces the amount of functional enzyme, thereby reducing net transport.

Na^+/H^+ exchange: J^{NaH}

Kinetics of Na^+/H^+ by Weinstein (*J.Gen.Physiol.*, 105:617, 1995): 2001): the transporter has a binding site that competes for Na^+ and H^+. The site also has a finite affinity for NH_4^+, permitting Na^+/NH_4^+ exchange.

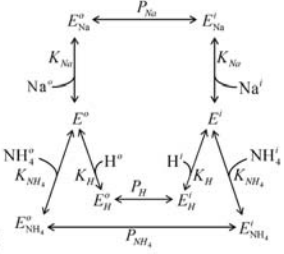

Ion binding is rapid relative to membrane translocation; binding is assumed in equilibriuim.

The model incorporates an internal modifier site (not shown) that enhances transport (increases P_{Na}, P_H and P_{NH4}) in response to a rise in intracellular $[H^+]$, an experimental finding in renal microvillous vesicles (Aronson *et al.*, *Nature* 299:161, 1983).

E. Characteristics of NHE-1 and NHE-3

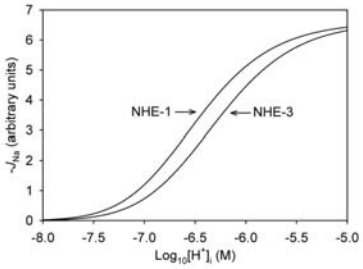

J_{Na} through Na^+/H^+ antiporter model of Weinstein (*J. Gen. Physiol.* 105:617, 1995).
NHE-3: $pK_i = 6.45$
NHE-1: $pK_i = 6.75$

Effect of internal modifier on Na^+/H^+ exchange

Intracellular acidification causes an increase in Na^+ flux via the exchanger (figure). The modifier is described by two parameters: f^M (= 2) is the factor rise in P_{Na}, K_I (= 10^{-6} M) is the $[H^+]_i$ producing half-maximal effect.

An hypothesis to be investigated is that isoforms of the Na/H differ in their values for K_I.

Other figure parameters:
$[Na^+]_o$ = 140 mM, $[Na^+]_i$ = 10 mM, $[NH_4]_{i,o}$ = 0, pH_o = 7.4

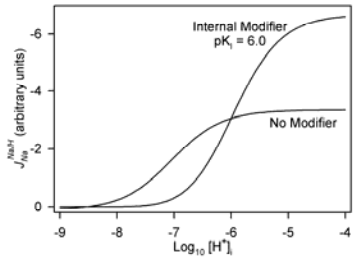

F. Steady-state Concentrations/Fluxes: Non-acid Species

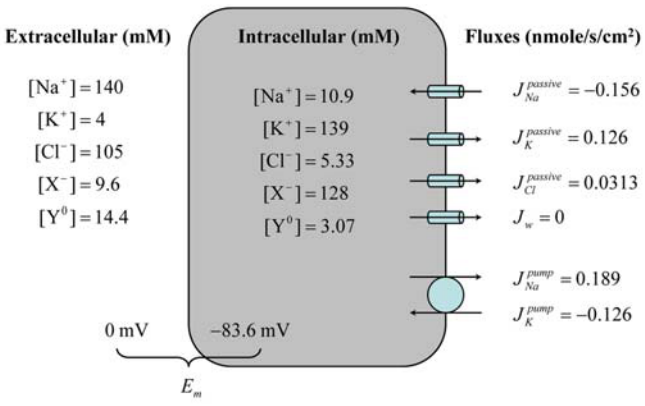

G. Steady-state Concentrations/Fluxes: Acid Species

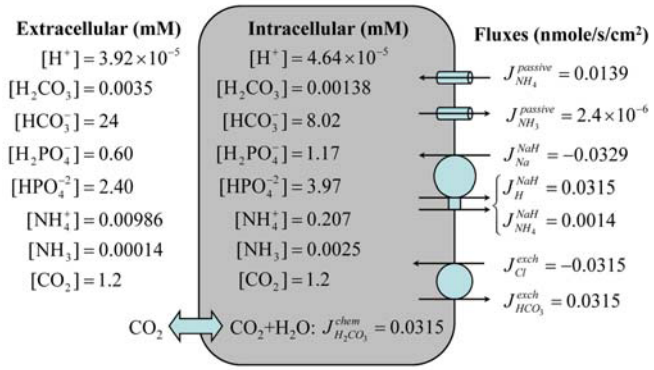

H. Summary of the Model

The model consists of 10 coupled differential equations, one for each of the following variables:

$$V, C^i_{Na^+}, C^i_{K^+}, C^i_{Cl^-}, C^i_{X^-}, C^i_{Y^0}, C^i_{H_T}, C^i_{B_{bicarb}}, C^i_{B_{phosphate}} \text{ and } C^i_{B_{ammonium}}$$

Initial conditions are specified, and the equations are integrated numerically as a function of time.

The equations are moderately stiff, owing mainly to the high water permeability (P_w) compared to the solute permeabilities; an adaptive ODE solver appropriate for stiff systems of equations (e.g., Gear's method) is used. The variables are solved to a relative tolerance of 10^{-6} or an absolute tolerance of 10^{-9}.

The model is coded in MATLAB®, and executes under its interactive programming environment.

III. RESULTS

A. Testing the Model: Simulated Hypercapnic Acidosis and NHE-1 vs. NHE-3

To test the hypothesis that differences between CO_2 chemosensitive and non-chemosensitive cells is due to different NHE isoforms, we compared the pH_i response to simulated hypercapnic acidosis using the model with the kinetics of the NHE-1 isoform and the NHE-3 isoform (Fig. 1). The model demonstrates that pH_i recovery is seen with both NHE isoforms, suggesting that the differences between CO_2 chemosensitive and non-chemosensitive cells are not due to different NHE isoforms.

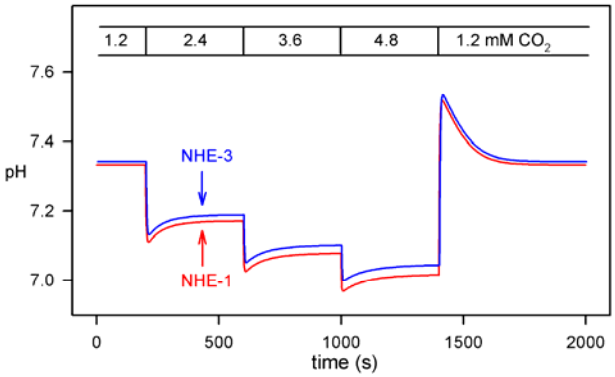

Figure 1. pH_i responses to simulated hypercapnic acidosis.

B. Testing the Model: Blockade of NHE (Amiloride Simulation)

To test the hypothesis that pH_i recovery is dependent upon NHE activity, we examined the effects of simulated blockade of NHE on pH_i recovery (Fig. 2). The model demonstrates that pH_i recovery is impaired in a dose-dependent manner with inhibition of NHE activity (simulation of amiloride effects), supporting a role for NHE in pH_i recovery.

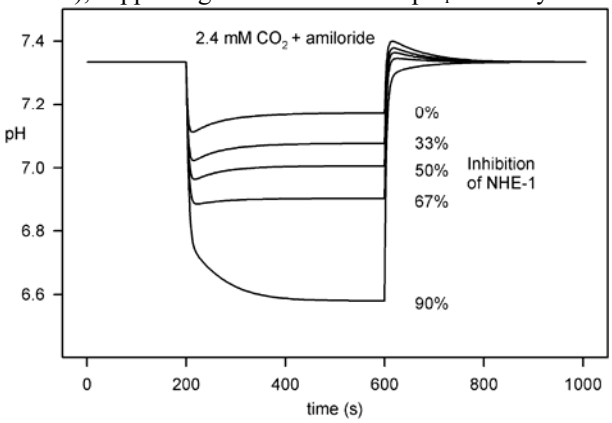

Figure 2. pH_i responses to simulated amiloride.

C. Testing the Model: Reduced NHE Activity

To test the hypothesis that lack of pH_i recovery in CO_2-chemosensitive cells is due to low NHE activity, we examined the effects of reduced NHE activity (*i.e.*, partial blockade of NHE) on pH_i recovery (Fig. 3). The model demonstrates that pH_i recovery is seen during low NHE activity, suggesting that other mechanisms are responsible. It should also be noted that the model demonstrates that reduced NHE activity is sufficient to decrease pH_i in the absence of increase CO_2 and the pH_i fall during simulated hypercapnia is exacerbated, suggesting that NHE activity plays an important role in maintaining basal pH_i.

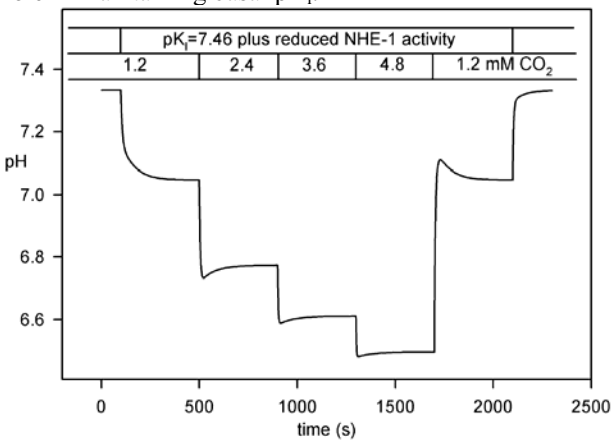

Figure 3. pH_i responses to simulated hypercapnic acidosis during reduced NHE activity.

D. Testing the Model: Regulation of NHE (Shift in Set-point (pK_I) of Internal Modifier Site

To test the hypothesis that lack of pH_i recovery in CO_2-chemosensitive cells is due to a shift in activation of the NHE, we examined the effects of shifting the activation

set-point of the internal modifier site of the NHE (Fig. 4). The model demonstrates that pH_i recovery is attenuated or abolished when the activation set-point of the internal modifier site of the NHE is shifted to a higher pH, suggesting that differences in regulation of the NHE may account for differences between CO_2-chemosensitive and non-chemosensitive cells.

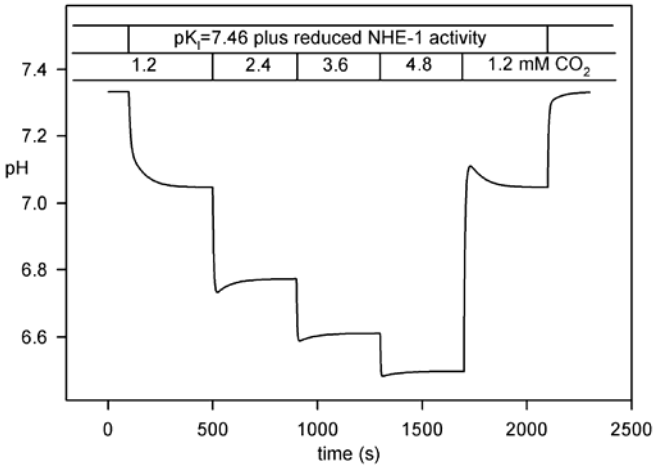

Figure 4. pH_i responses to simulated hypercapnic acidosis following a shift in the activation set-point of the NHE. To correct for the fall in basal pH_i, NHE activity was also reduced.

E. Testing the Model: Effects of Blockade of NHE Following Shift in pK$_I$ (CO_2-chemosensitive Cell)

To further evaluate the role of NHE in the blunted pH_i recovery response identified following a shift in activation set-point of the internal modifier site of the NHE (*i.e.*, the CO_2-chemosensitive cell), we examined the effects of simulated blockade of NHE on pH_i after shifting the activation set-point (Fig. 5). The model demonstrates that pH_i recovery is not observed during simulated amiloride in the CO_2-sensitive cell but is seen with sustained hypercapnia following removal of amiloride, similar to the experimental data of Ritucci et al. [1].

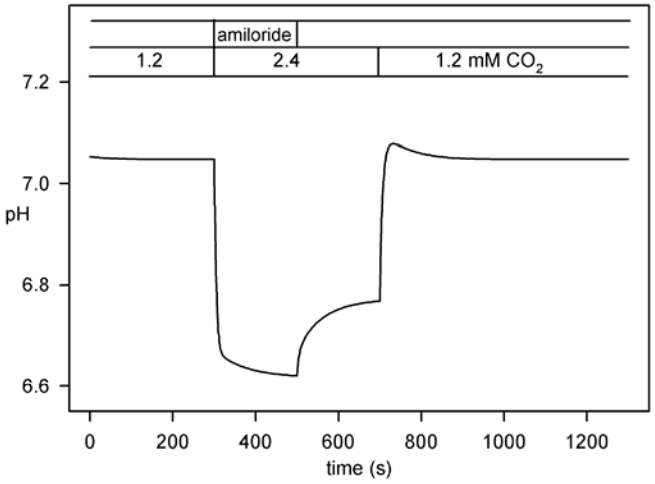

Figure 5. pH_i responses to simulated hypercapnic acidosis and blockade of NHE in a CO_2-chemosentitive cell (*i.e.*, cell with shift in activation set-point of the NHE).

IV. Summary And Conclusions

In response to simulated hypercapnia, the model incorporating either the NHE-1 or NHE-3 isoform show pH_i recovery that is dependent on NHE (based on simulation of amiloride effects); thus, different NHE isoforms cannot explain the differences between CO_2-chemosensitive and non-chemosensitive cells. In addition, pH_i recovery is dependent upon NHE activity, and inhibition of NHE is sufficient to decrease pH_i in the absence of increased CO_2 and it enhances the fall in pH_i during simulated hypercapnia. Finally, the model demonstrates that differences in pH_i regulation in CO_2-chemosensitive versus non-chemosensitive neurons may be dependent upon differences in the set-point of the internal modifier site of the NHE, which can be differentially regulated in the different NHE isoforms by numerous signaling pathways (e.g., activation of PKA and PKC, increased levels of cAMP, cGMP, and $[Ca^{2+}]_i$). Additional H^+ extrusion pathways as well as the role of the AE need to be explored to identify other mechanisms involved in pH_i regulation in CO_2 chemosensitive neurons.

Acknowledgment

This project was initiated as part of a graduate course entitled *Mathematical Modeling of Physiological and Biophysical Systems*. The course was developed with financial support from a NIH/NIDDK Curriculum Development Grant.

References

[1] N.A. Ritucci, J.B. Dean, and R.W. Putnam, "Intracellular pH response to hypercapnia in neurons from chemosensitive areas of the medulla" *Am J Physiol* 273: R433-441, 1997.

[2] N.A. Ritucci, L. Chambers-Kersh, J.B. Dean, and R.W. Putnam, "Intracellular pH regulation in neurons from chemosensitive and nonchemosensitive areas of the medulla" *Am J Physiol* 275: R1152-1163, 1998.

[3] R.W. Putnam, "Intracellular pH regulation of neurons in chemosensitive and nonchemosensitive areas of brain slices" *Respir Physiol* 129: 37-56, 2001.

[4] M. Wiemann and D. Bingmann, "Ventrolateral neurons of medullary organotypic cultures: intracellular pH regulation and bioelectric activity" *Respir Physiol* 129: 57-70, 2001.

[5] M. Wiemann, J.R. Schwark, U. Bonnet, H.W. Jansen, S. Grinstein, R.E. Baker, H.J. Lang, K. Wirth, and D. Bingmann, "Selective inhibition of the Na^+/H^+ exchanger type 3 activates CO_2/H^+-sensitive medullary neurons" *Pflugers Arch* 438: 255-262, 1999.

[6] S.C. Hempleman and R.G. Posner, "CO_2 transduction mechanisms in avian intrapulmonary chemoreceptors: experiments and models" *Respir Physiol Neurobiol* 144: 203-214, 2004.

[7] H. Chang and T. Fujita, "A numerical model of acid-base transport in rat distal tubule" *Am J Physiol Renal Physiol* 281: F222-243, 2001.

[8] A.M. Weinstein, "A kinetically defined Na^+/H^+ antiporter within a mathematical model of the rat proximal tubule" *J Gen Physiol* 105: 617-641, 1995.

[9] P.S. Aronson, M.A. Suhm, and J. Nee, "Interaction of external H^+ with the Na^+/H^+ exchanger in renal microvillus membrane vesicles" *J Biol Chem* 258: 6767-6771, 1983.